Nat. Hazards Earth Syst. Sci., 13, 1579–1593, 2013
www.nat-hazards-earth-syst-sci.net/13/1579/2013/
doi:10.5194/nhess-13-1579-2013

Natural Hazards and Earth System Sciences
Open Access

Effectiveness of modified pushover analysis procedure for the estimation of seismic demands of buildings subjected to near-fault ground motions having fling step

A. Mortezaei[1] **and H. R. Ronagh**[2]

[1]Department of Civil Engineering, Semnan Branch, Islamic Azad University, Semnan, Iran
[2]School of Civil Engineering, The University of Queensland, Brisbane, Australia

Correspondence to: A. Mortezaei (a.mortezaei@semnaniau.ac.ir)

Received: 27 May 2012 – Published in Nat. Hazards Earth Syst. Sci. Discuss.: –
Revised: – Accepted: 3 May 2013 – Published: 19 June 2013

Abstract. Near-fault ground motions with long-period pulses have been identified as being critical in the design of structures. These motions, which have caused severe damage in recent disastrous earthquakes, are characterized by a short-duration impulsive motion that transmits large amounts of energy into the structures at the beginning of the earthquake. In nearly all of the past near-fault earthquakes, significant higher mode contributions have been evident in building structures near the fault rupture, resulting in the migration of dynamic demands (i.e. drifts) from the lower to the upper stories. Due to this, the static nonlinear pushover analysis (which utilizes a load pattern proportional to the shape of the fundamental mode of vibration) may not produce accurate results when used in the analysis of structures subjected to near-fault ground motions. The objective of this paper is to improve the accuracy of the pushover method in these situations by introducing a new load pattern into the common pushover procedure. Several pushover analyses are performed for six existing reinforced concrete buildings that possess a variety of natural periods. Then, a comparison is made between the pushover analyses' results (with four new load patterns) and those of FEMA (Federal Emergency Management Agency)-356 with reference to nonlinear dynamic time-history analyses. The comparison shows that, generally, the proposed pushover method yields better results than all FEMA-356 pushover analysis procedures for all investigated response quantities and is a closer match to the nonlinear time-history responses. In general, the method is able to reproduce the essential response features providing a reasonable measure of the likely contribution of higher modes in all phases of the response.

1 Introduction

While nonlinear response history analysis is the most powerful and most difficult procedure for the estimation of seismic demands, current structural engineering practice uses a nonlinear static procedure otherwise known as pushover analysis. The method is relatively simple and considers post-elastic behaviour. It, however, involves certain simplifications that result in approximations in the seismic demand predictions, in particular for seismic events in which significant higher mode contributions do exist, such as near-fault earthquakes having fling step.

The near-fault region of an earthquake can be defined as the area in close proximity to the fault rupture. Besides strong shaking, the characteristics of near-fault ground motions are linked to the fault geometry and the orientation of the travelling seismic waves (Somerville, 2000). Figure 1 portrays the three zones of directivity, with the star representing the epicentre and the black line indicating the fault rupture. The rupture directivity pulse is oriented in the strike-normal direction and the static ground displacement (fling step) is oriented parallel to the fault strike. Fling step is a result of the evolution of residual ground displacement due to tectonic deformation associated with rupture mechanism. This phenomenon is characterized by a unidirectional large amplitude velocity pulse and a monotonic step in the displacement time history (Somerville, 2000). It arises the strike parallel direction for strike slip faults or in the strike normal direction for dip-slip faults. In general, the permanent displacement is considered as the pseudo-static deformation and its frequency is smaller than that of the forward directivity pulse.

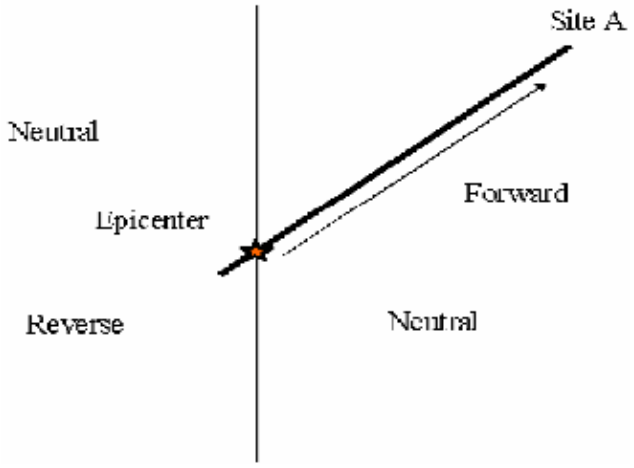

Fig. 1. Zones of directivity (Somerville, 2000).

The velocity and displacement time histories of typical near-fault ground motions having fling step (such as the Sakarya record of the 1999 Kocaeli earthquake) are compared to those histories of ordinary far-fault motion (such as the Taft record of the 1952 Kern County earthquake) in Fig. 2. This figure shows that the fault-parallel component of the Sakarya record exhibits apparent tectonic deformation at the end of the displacement time history that is a typical signature of the fling step.

In this study, it is intended to improve the accuracy of the pushover procedure and to ascertain its validity and applicability for near-fault earthquake analysis by introducing new lateral load configurations into the procedure. The results from these pushover analyses are checked against full nonlinear time-history analysis results in order to prove their validity. The earthquake recordings used for the analysis are carefully compiled so as to reflect characteristics typical of near-fault records having fling step.

2 Background

Pushover analysis is essentially the nonlinear incremental-iterative solution of the equilibrium equation $\mathbf{KU} = \mathbf{P}$ in a finite element formulation, where **K** is the nonlinear stiffness matrix, **U** is the displacement vector and **P** is a predefined load vector (Fig. 3) applied laterally over the height of the structure in relatively small load increments. The analysis is often performed in two stages: load controlled and displacement controlled. The former stage occurs prior to significant yielding and the latter after significant yielding where the force-displacement curve does not ascend as quickly. For the displacement controlled part, at the end of each iteration the reaction vector ($\mathbf{P}^e$) of the structure is calculated from the assemblage of all finite element contributions. The out-of-balance forces are then iteratively re-applied until convergence to a specified tolerance is reached:

$$\Delta U = [K_T]^{-1} . \left(\lambda . P_0 - P^e\right) \quad (1)$$

Where:

- ΔU is the calculated displacement increment within an iteration.
- K_{T} is the current nonlinear stiffness matrix.
- λ is the load factor within the corresponding load increment.
- P_0 is the initial load.
- P^{e} is the equilibrated load of the previous iteration.

$$P^e = \sum \int_{\mathrm{V}} \mathrm{B}^{\mathrm{T}} . \sigma_{\mathrm{NL}} . \mathrm{dV} \quad (2)$$

- B is the strain-displacement matrix of each element.
- σ_{NL} is the element nonlinear stress vector as determined by its material constitutive law.

The procedure continues either until a predefined limit state is reached or until structural collapse is detected. This target limit state may be the deformation expected for the design earthquake, in the case of designing a new structure, or the drift corresponding to structural collapse for assessment purposes. Generally, this procedure allows the tracing of the sequence of yielding and failure at the member and structure level, as well as the progress of the overall capacity curve of the structure (Fig. 4).

The use of inelastic static analysis (pushover) in earthquake engineering is traced to the work of Gulkan and Sozen (1974), where a single degree of freedom system is derived to represent the multi-degree of freedom structure via an equivalent structure.

Since the publication of FEMA (Federal Emergency Management Agency)-356, pushover methods have been the subject of several studies (Krawinkler and Seneviratna, 1998; Tso and Moghadam, 1998; Satyarno et al., 1998; Wight et al., 1999; Mwafy and Elnashai, 2001). An adaptive procedure is described in the paper by Bracci et al. (1997). The procedure was implemented in the dynamic analysis package IDARC (Inelastic Damage Analysis of Reinforced Concrete) (Kunnath et al., 1992) and was proven to provide accurate results for the structure considered. However, numerical tests conducted by Lefort (2000) showed that the above procedure grossly underestimated the strength, compared to inelastic dynamic analysis using IDARC. The drawbacks in pushover methods using invariant FEMA-based lateral load patterns have led to alternative pushover strategies. The multi-mode pushover (Sasaki et al., 1998) tries to incorporate higher modes by considering multiple pushover curves

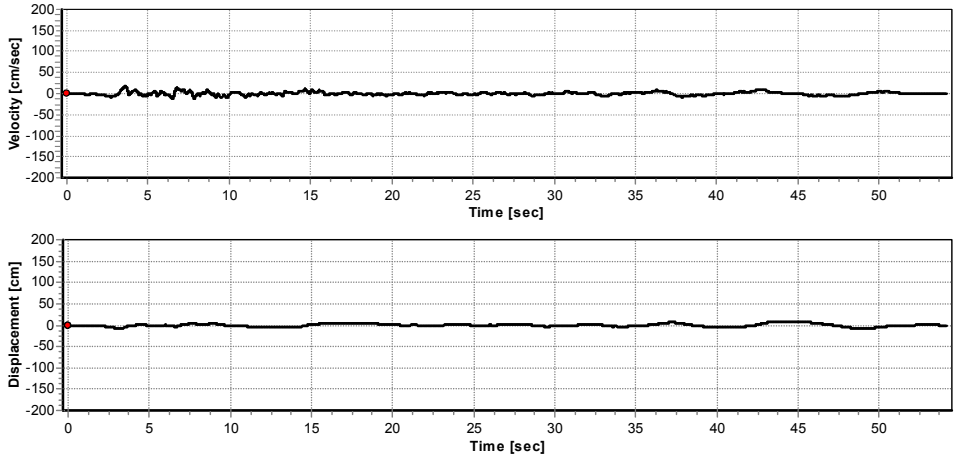

(a) Taft record of 1952 Kern County earthquake

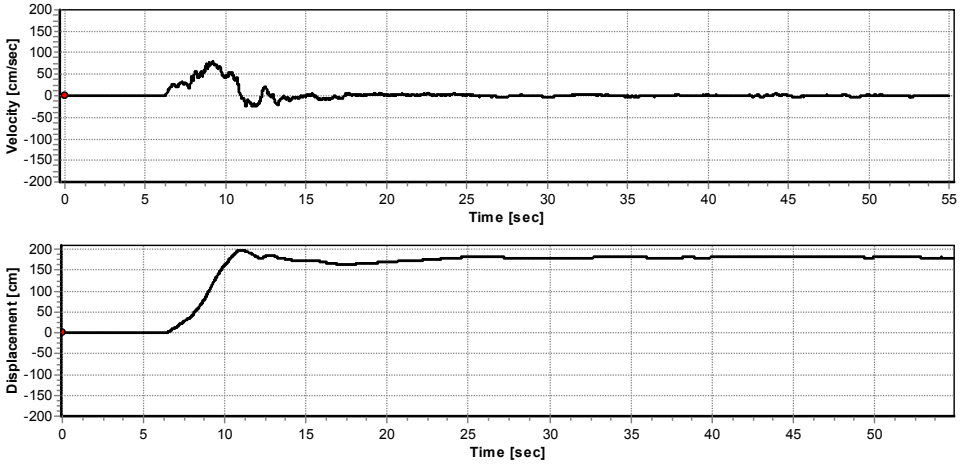

(b) Sakarya record of 1999 Kocaeli earthquake

Fig. 2. Typical velocity and displacement time histories of **(a)** far-fault and **(b)** near-field (fling step) ground motions.

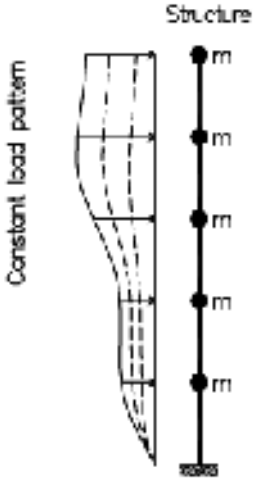

Fig. 3. Load pattern in pushover analysis.

derived from different modal force patterns. The adaptive pushover method developed by Gupta and Kunnath (2000) uses a varying load pattern that pushes and pulls the structure by combining modes at different stiffness states of the structure. Chopra and Goel (2002) proposed a modal pushover technique that combines the response of individual modal demands with reasonable success.

The recently developed modal pushover analysis (MPA) for estimating seismic demands on buildings has been shown to be a significant improvement over the pushover analysis procedures currently used in structural engineering practice. None of the current invariant force distributions account for the contribution of higher modes to the response or for the redistribution of inertial forces because of structural yielding.

Kalkan and Kunnath (2006) proposed a new pushover analysis procedure derived through adaptive modal combinations (AMC) for evaluating the seismic performance of building structures. The AMC procedure accounts for higher mode effects by combining the response of individual modal

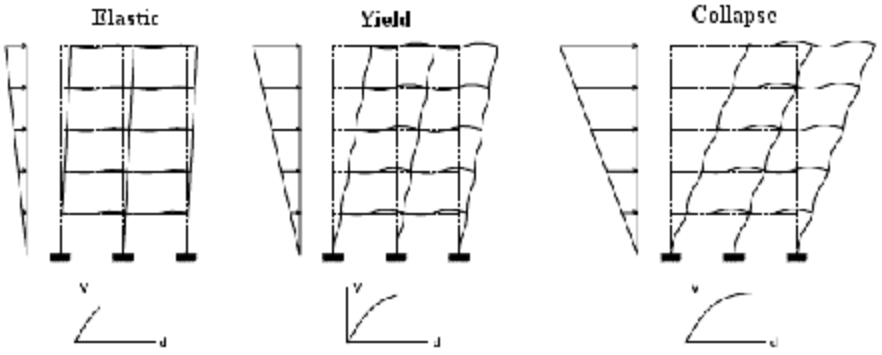

Fig. 4. Yielding sequence through conventional pushover analysis.

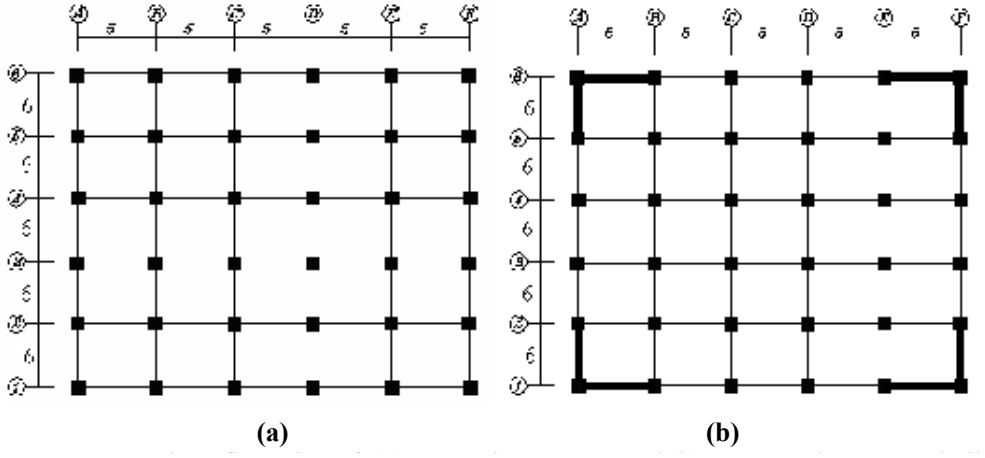

Fig. 5. Structural configuration of **(a)** 3-, 6- and 10-storey; and **(b)** 14-, 16- and 19-storey buildings.

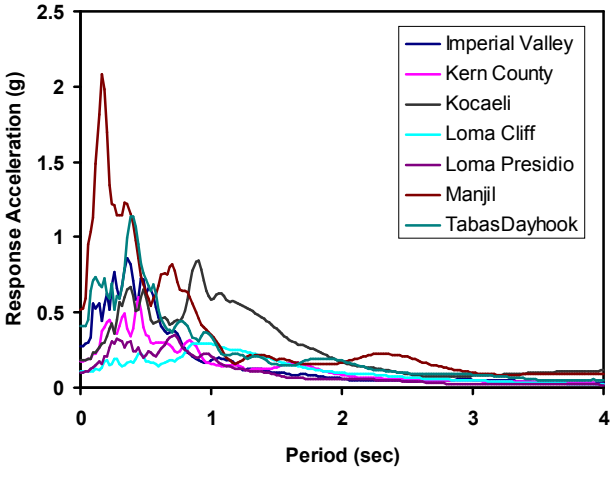

Fig. 6. Elastic acceleration response spectra of far-fault ground motion recordings used in the evaluation of each building.

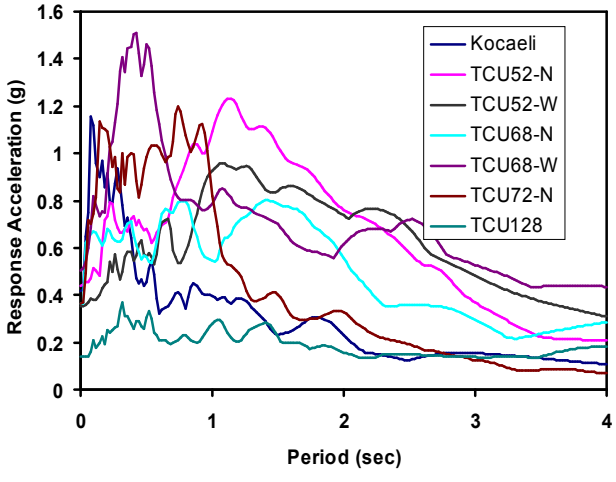

Fig. 7. Elastic acceleration response spectra of near-fault ground motion recordings used in the evaluation of each building.

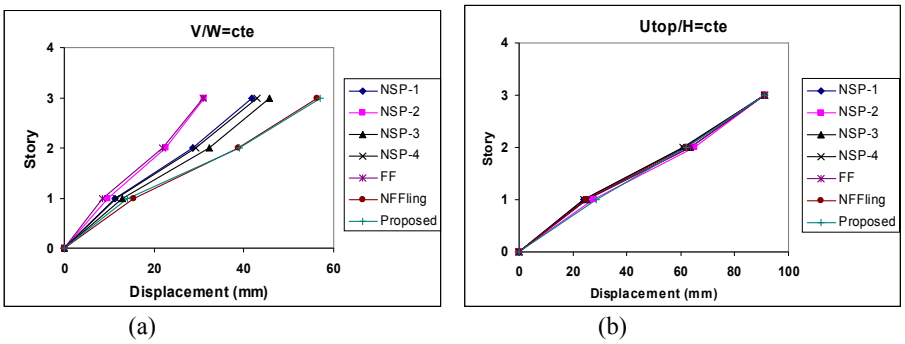

(a) (b)

Fig. 8. Peak displacement profiles for the 3-storey building with **(a)** V/W=cte, **(b)** U_{top}/H=cte.

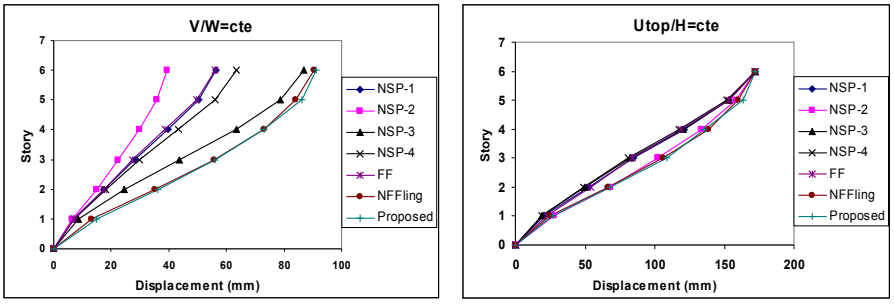

(a) (b)

Fig. 9. Peak displacement profiles for the 6-storey building with **(a)** V/W=cte, **(b)** U_{top}/H=cte.

pushover analyses and incorporates the effects of varying dynamic characteristics during the inelastic response via its adaptive feature. A novel feature of the procedure is that the target displacement is estimated and updated dynamically during the analysis by incorporating energy-based modal capacity curves in conjunction with constant-ductility capacity spectra. Turker and Irtem (2007) presented an effective multi-modal and adaptive pushover analysis (PA) procedure for the determination of earthquake response of building-type structures affected from the higher modes.

In the traditional pushover, both the force distribution and the target displacement are based on the assumption that the response is controlled by a fundamental mode that remains unchanged throughout. Such invariant force distributions cannot account for the redistribution of inertia forces caused by structural yielding and the associated changes in the vibration properties, including the increase of higher mode participation. In order to overcome such drawbacks, adaptive pushover techniques were proposed. In order to investigate the effectiveness of these new pushover schemes in assessing bridges subjected to seismic action, Pinho et al. (2007) carried out an analytical parametric study on a suite of continuous multi-span bridges. Mao et al. (2008) presented an improved MPA procedure to estimate the seismic demands of structures, considering the redistribution of inertia forces after the structure yields. This improved procedure is verified with numerical examples of 5-, 9- and 22-storey buildings. It was concluded that the improved MPA procedure is more accurate than either the pushover analysis procedure or the MPA procedure. In addition, the proposed procedure avoids a large computational effort by adopting a two-phase lateral force distribution. Huang and Kuang (2009) investigated the applicability of pushover analysis for seismic evaluation of medium-to-high-rise shear-wall structures. The results of the analysis were compared with those from the pushover procedure. It was shown that pushover analysis generally underestimates interstorey drifts and rotations, in particular those at upper stories of buildings, and overestimates the peak roof displacement at the inelastic deformation stage. It was shown that neglecting higher mode effects in the analysis will significantly underestimate the shear force and overturning moment.

Several researchers (Chopra and Goel, 2002; Jan et al., 2004) have proposed enhanced pushover procedures to account for higher mode effects while retaining the simplicity of invariant load patterns. These improved procedures utilize the concept of modal combinations, either through a single pushover analysis where the load vectors reflect the contributions from each elastic mode-shape considered, or through multiple pushover analyses using invariant load patterns based on elastic mode shapes where the contribution from each mode is combined at the end.

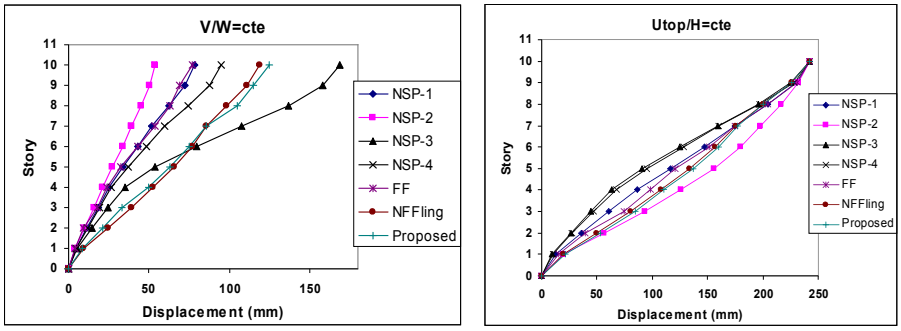

(a) (b)

Fig. 10. Peak displacement profiles for the 3-storey building with **(a)** V/W=cte, **(b)** U_{top}/H=cte.

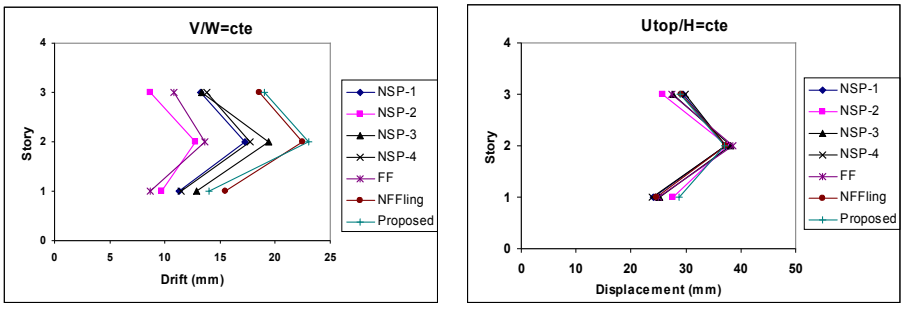

(a) (b)

Fig. 11. Interstorey drift for 3-storey building with **(a)** V/W=cte, **(b)** U_{top}/H=cte.

All these enhanced procedures have been shown to provide improved estimates of interstorey drift values compared to conventional nonlinear static-procedures (NSPs) using inverted triangular, uniform, or other lateral load patterns based on direct modal combination.

Amongst pushover analysis procedures that are able to consider the higher mode effects, three procedures are most notable: modal pushover analysis – MPA (Chopra and Goel, 2002), adaptive modal combination – AMC procedure (Gupta and Kunnath, 2000) and incremental response spectrum analysis – IRSA (Aydinoglu, 2003, 2004). These procedures are able to estimate the nonlinear deformation demands under a given earthquake and are therefore suitable for use in a deformation-based seismic evaluation/design process.

The standard response spectrum analysis (RSA) for elastic buildings is reformulated as an MPA. The peak response of the elastic structure due to its n-th vibration mode can be exactly determined by pushover analysis of the structure subjected to lateral forces distributed over the height of the building according to $\mathbf{S}_n = \mathbf{m}\varphi_n$, where m is the mass matrix and φ_n its n-th mode, and the structure is pushed to the roof displacement determined from the peak deformation of the n-th-mode elastic SDF system. Combining these peak modal responses by the modal combination rule leads to the MPA procedure.

The AMC procedure derives its fundamental scheme from the adaptive pushover procedure of Gupta and Kunnath (2000) by recognizing the need to modify applied lateral loads as the system responds to the applied earthquake load.

In this study, the inability of pushover methods to predict demands for near-fault ground motions having fling step is demonstrated and a new procedure for predicting the nonlinear behaviour of RC buildings is proposed.

3 Description of the proposed procedure

In practical applications it is required that inelastic spectral displacement is calculated in a simple manner, preferably using the code-specified smoothed response spectrum, where the well-known *equal displacement rule* can be effectively utilized. According to this simple and well-known rule, spectral displacement of an inelastic SDOF (single degree of freedom) system and that of the corresponding elastic system are assumed to be practically equal to each other, provided that the effective-initial period of the former is longer than the *characteristic period* of the earthquake. The characteristic period is approximately defined as the transition period from the constant acceleration segment to the constant velocity segment of the response spectrum. For periods shorter than the characteristic period, elastic spectral displacement is

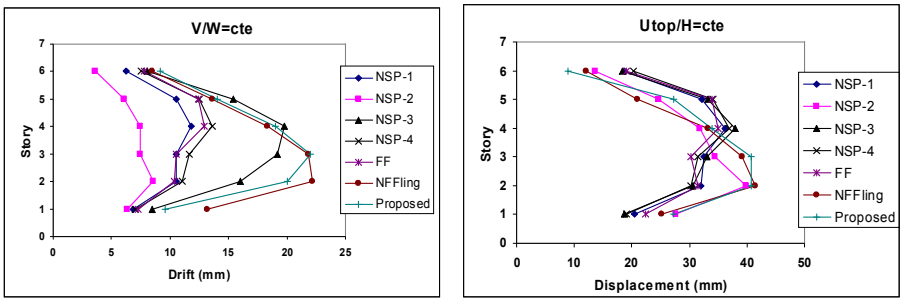

Fig. 12. Interstorey drift for 6-storey building with **(a)** V/W=cte, **(b)** U_{top}/H=cte.

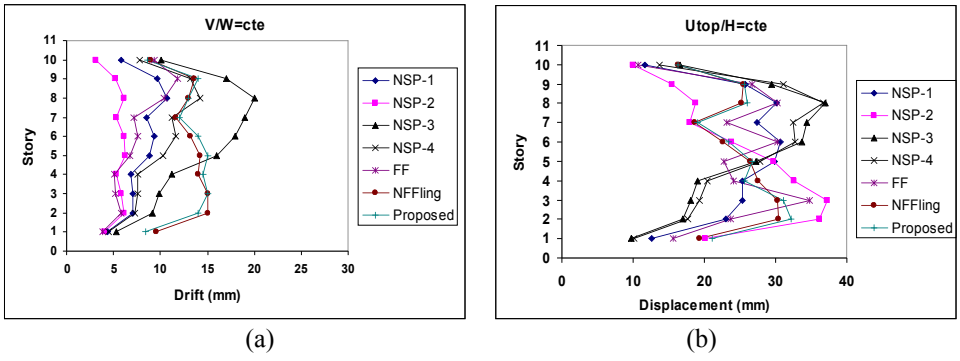

Fig. 13. Interstorey drift for 10-storey building with **(a)** V/W=cte, **(b)** U_{top}/H=cte.

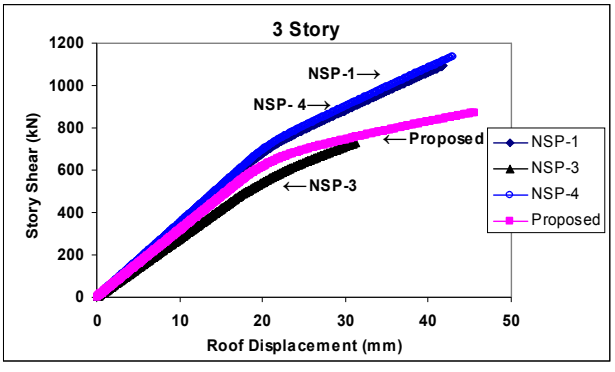

Fig. 14. Base shear vs roof drift response using different lateral load profiles for 3-storey building.

appropriately amplified. But, an exception to this commonly accepted rule is the near-fault ground motions with fling step effect. Hence, to solve this problem, in the proposed method, a new procedure for determination of lateral load distribution with respect to the near-fault ground motions with fling step effect is proposed.

Analysis steps of the proposed procedure, which are detailed fully in Mortezaei (2010), are summarized below:

1. Run a linear RSA with a sufficient number of modes by considering the instantaneous second-order stiffness matrix corresponding to the current plastic hinge configuration.

2. Determine the moment–curvature relationships based on the conditions of beams and columns using the material and cross-sectional properties.

3. Determine the response quantities (internal forces, nodal displacements, etc.) for gravity loads. Consider the effects of the axial forces on element stability functions. Check whether or not any plastic section occurs in the structural system due to gravity loads.

4. Idealize the structural system stiffness matrix for required degrees of freedom and obtain the dynamic stiffness matrix. Perform free vibration analysis, determine the modal properties of the structural system with plastic sections, and then determine the unit modal lateral load distribution for all of the considered modes.

5. Apply unit modal load distributions to the system (modified due to plastic behaviour) independently and obtain modal response quantities for each mode considered in the analysis. Then, combine modal quantities using the appropriate modal combination rule, and determine the

combined response quantities due to the unit load increment. Assign the sign of effective mode in the current step to the combined response quantities in order to use it in the yield conditions.

6. Determine the location of the plastic section and the related load increment factor at the current step by using yield conditions for all critical sections. Then, obtain response quantities at the current step.

7. Modify properties of the structural system due to plastic behaviour and repeat the process until the instability limit state of the system is reached. When the structural system reaches this limit state, the determinant of the stiffness matrix of the system modified due to plastic behaviour is negative or zero, that is, the stiffness matrix loses its positive definite attribute.

The proposed methodology integrates the inherent advantages of the capacity spectrum method and the modal pushover procedure, and at the same time eliminates the need to pre-estimate the target displacement.

4 Description of buildings used for evaluation

Six existing reinforced concrete special moment-resisting frame buildings of 3, 6, 10, 14, 16 and 19 stories were selected as representative case studies to evaluate their seismic demands when subjected to near-fault ground motions having fling step, and to compare the respective responses to typical far-fault ground motions. These buildings were designed in compliance to the Iranian Code of Practice for Seismic Resistant Design of Buildings (2005). The buildings with three, six and ten stories possess a moment-resisting frame system and the buildings with fourteen, sixteen and nineteen stories, a wall-frame system. The rectangular plan of all buildings measures 30 m × 25 m. The floor plans are shown in Fig. 5. The columns are embedded into grade beams and anchored to the top of the pile cap, essentially restraining displacements and rotations in all directions. The buildings are assumed to be fixed at the base with a damping ratio of 5 % in all modes, and the floors are rigid diaphragms with infinite in-plane stiffness. The sections of structural elements are square and rectangular and their dimensions are changed at different stories. The slab thickness is 10 cm. For the sake of clarity, the column and beam dimensions and reinforcement of the 10-storey building have been listed in Tables 1 and 2. Storey heights of buildings are assumed to be constant with the exception of the ground storey. The modulus of elasticity (Young's modulus) $E = 30$ KPa, Poisson's ratio $\nu = 0.20$ and the mass density $\rho = 24\,\mathrm{kN\,m^{-3}}$ are assumed in all models. The uniaxial strength for nonlinear modelling of the concrete is considered to be 35 MPa. The rebar is modelled as steel with yield strength of 400 MPa and an ultimate strength of 600 MPa.

Permanent and imposed loads are assumed to be: dead load of storey level, 5.5 KPa; dead load of roof, 6 KPa; dead load of partitions, 1 KPa; dead load of external walls, 2.5 KPa; live load of storey levels, 2 KPa; and live load of roof, 1.5 KPa.

5 Comparative study of seismic demands

The six buildings described in the previous section are evaluated using nonlinear static and nonlinear dynamic procedures to compare the resulting demands. In the case of static approaches, the following lateral load configurations were considered:

NSP-1

The inverse triangular distribution, often suggested in building codes, considers that the structure is subjected to a linear distribution of the acceleration throughout the building height. The force increment at each step for storey "i" is calculated according to

$$\Delta F_i = \frac{W_i h_i}{\sum_{l=1}^{N} W_l h_l} \Delta V_\mathrm{b}\,, \tag{3}$$

where W_i and h_i are the storey weight and the storey elevation, respectively, and ΔV_b is the increment of the building base shear.

NSP-2

The uniform distribution considers a constant distribution of the lateral forces throughout the height of the building, regardless of the storey weights. The force increment at each step for storey "i" is given by

$$\Delta F_i = \frac{\Delta V_\mathrm{b}}{N}, \tag{4}$$

where ΔV_b is the increment in the base shear of the structure, and N is the total number of stories in the building.

NSP-3

The generalized power distribution was introduced to consider different variation of the storey accelerations with the storey elevation. This distribution was introduced to capture different modes of deformation, and the influence of higher modes in the response. The force increment at floor "i" is calculated according to

$$F_i = \frac{W_i h_i^K}{\sum_{j=1}^{n} W_j h_j^K} V, \tag{5}$$

where k is the parameter that controls the shape of the force distribution.

Table 1. Dimensions and amount of reinforcement of columns and shear walls in the 10-storey building.

Building	Storey	Corner column		Perimeter column		Internal column		Shear wall
		Dim. (cm)	Reo. $(mm)^2$	Dim. (cm)	Reo. $(mm)^2$	Dim. (cm)	Reo. $(mm)^2$	Thickness (cm)
10 storey	**1**	60 × 60	2100	60 × 60	1880	60 × 60	1930	–
	2	60 × 60	1200	60 × 60	1200	60 × 60	1200	–
	3	60 × 60	1200	60 × 60	1200	60 × 60	1200	–
	4	60 × 60	1200	60 × 60	1200	60 × 60	1200	–
	5	50 × 50	910	50 × 50	1335	50 × 50	950	–
	6	50 × 50	840	50 × 50	910	50 × 50	840	–
	7	50 × 50	840	50 × 50	900	50 × 50	840	–
	8	40 × 40	775	40 × 40	1070	40 × 40	840	–
	9	40 × 40	600	40 × 40	880	40 × 40	600	–
	10	40 × 40	600	40 × 40	880	40 × 40	600	–

Table 2. Dimensions and amount of reinforcement of beams in 10 storey-building.

Storey	Beams of external frames						Beams of internal frames					
	Type 4			Type 3			Type 2			Type 1		
	Dim. (cm) h × w	Reo. (mm^2)		Dim. (cm) h × w	Reo. (mm^2)		Dim. (cm) h × w	Reo. (mm^2)		Dim. (cm) h × w	Reo. (mm^2)	
		Bot.	Top		Bot.	Top		Bot.	Top		Bot.	Top
1	60 × 50	1316	1664	60 × 50	1108	1583	60 × 50	1176	1670	60 × 50	1104	1593
2	60 × 50	1685	2071	60 × 50	1488	1972	60 × 50	1532	2093	60 × 50	1484	1981
3	60 × 50	1728	2141	60 × 50	1566	2054	60 × 50	1568	2176	60 × 50	1562	2059
4	60 × 50	1764	2181	60 × 50	1564	2043	60 × 50	1600	2223	60 × 50	1557	2055
5	50 × 45	1484	1931	50 × 45	1276	1823	50 × 45	1298	1965	50 × 45	1270	1835
6	50 × 45	1393	1860	50 × 45	1221	1770	50 × 45	1203	1903	50 × 45	1214	1778
7	50 × 45	1287	1737	50 × 45	1076	1607	50 × 45	1103	1779	50 × 45	1066	1625
8	40 × 40	947	1424	40 × 40	711	1334	40 × 40	738	1449	40 × 40	702	1352
9	40 × 40	665	1157	40 × 40	529	1100	40 × 40	570	1190	40 × 40	533	1110
10	40 × 40	495	760	40 × 40	473	727	40 × 40	502	773	40 × 40	492	757

The recommended value for k may be calculated as a function of the fundamental period of the structure (T):

$$\begin{aligned} &k = 1.0 \quad \text{for } T \le 0.5\,\text{s}, \\ &k = 2.0 \quad \text{for } T \ge 2.5\,\text{s}, \\ &k = 1 + \tfrac{T-0.5}{2} \quad \text{otherwise.} \end{aligned} \tag{6}$$

Nevertheless, any value for k may be used to consider different acceleration profiles. Note that $k = 0$ produces a constant variation of the acceleration, while $k = 1$ produces a linear variation (inverted triangle distribution), and $k = 2$ yields a parabolic distribution of storey accelerations.

NSP-4

The modal adaptive distribution differs markedly from all previous cases in that the storey force increments are not constant. A constant distribution throughout the incremental analysis will force the structure to respond in a certain form. Often the distribution of forces is selected considering force distributions during an elastic response; however, it is clear that when the structure enters the inelastic range, the elastic distribution of forces may not be applicable anymore. If the pushover forces are not modified to account for the new stiffness distribution, the structure is forced to respond in a way that may considerably differ from what an earthquake may impose on the structure.

The modal adaptive distribution was developed to capture the changes in the distribution of lateral forces. Instead of a polynomial distribution, the mode shapes of the structure are considered. Since the inelastic response of the structure will change the stiffness matrix, the mode shapes will also be affected, and a distribution proportional to the mode shapes will capture this change. If the fundamental mode is considered, the increment in the force distribution is calculated according to

$$\Delta F_i = \frac{W_i \varphi_{i1}}{\sum_{i=1}^{N} W_i \varphi_{i1}} V_\mathrm{b} - F_i^{\mathrm{old}} , \tag{7}$$

where φ_{i1} is the value of the first mode shape at storey "i", V_b is the new base shear of the structure, and F_i^{old} is the force at floor "i" in the previous loading step.

The modal adaptive distribution may be extended to consider the contribution from more than one mode. In this case

Table 3. Target displacement and periods of buildings.

Buildings	3 storey	6 storey	10 storey	14 storey	16 storey	19 storey
Period (s)	0.74	1.16	1.5	1.88	2.24	2.92
Response coefficient	1.92	1.43	1.20	1.03	0.92	0.77
Target displacement (cm)	9.1	17.2	24.2	32.5	41.3	58.7

Table 4. Far-field ground motion database.

NO.	Earthquake	Year	Station	Comp.	M_w	Dis. (km)	PGA (g)	PGV ($cm\,s^{-1}$)	PGD (cm)
1	Kern County	1952	Taft	111	7.4	81	0.17	17.47	8.83
2	Tabas	1978	Dayhook	TR	7.4	107	0.4	26.17	9.1
3	Imperial Valley	1979	Calexico	225	6.5	90.6	0.27	21.23	8.98
4	Loma Prieta	1989	Presidio	000	6.9	83.1	0.099	12.91	4.32
5	Loma Prieta	1989	Cliff House	90	6.9	84.4	0.107	19.78	5.06
6	Manjil	1990	Abbar	L	7.3	74	0.51	42.46	14.92
7	Kocaeli	1999	Ambarli	90	7.4	78.9	0.18	33.22	25.84

the mode shapes are combined using the Square Root of the Sum of the Squares (SRSS) method and scaled according to their modal participation factor. The incremental force at storey "i" is calculated according to

$$\Delta F_i = \frac{W_i \left[\sum_{j=1}^{nm} \left(\varphi_{ij}\Gamma_j\right)^2\right]^{1/2}}{\sum_{l=1}^{n} W_l \left[\sum_{j=1}^{nm} \left(\varphi_{lj}\Gamma_j\right)^2\right]^{1/2}} V_b - F_i^{old}\ , \quad (8)$$

where Φ_{ij} is the value of mode shape "j" at storey "i", Γj is the modal participation factor for mode "j", V_b is the new base shear of the structure, and F_i^{old} is the force at floor "i" in the previous loading step.

5.1 Target displacement

Each of the six building models was subjected to the four lateral load patterns enumerated above, until the roof reached a specified target displacement. The target displacements were computed using the provisions in FEMA-356 (2000). As an empirical method, target displacement can be calculated according to Eq. (9):

$$\delta_t = C_0 C_1 C_2 C_3 S_a \frac{T_e^2}{4\pi^2} g, \quad (9)$$

where

- T_e: fundamental effective period of building.
- C_0: corrective coefficient for relation between spectral displacement of a single degree of freedom system and roof displacement of a multi-degree freedom system.
- C_1: coefficient of stiffness and structural element strength degradation for the sake of plastic behaviour.
- C_2 and C_3: coefficients that are calculated according to the FEMA-356.
- S_a: spectral acceleration.

Using this, target displacements of buildings were calculated as shown in Table 3.

6 Ground motion database

The validity of pushover procedures based on the four invariant load distributions is examined using the results of nonlinear time-history analyses as a benchmark. The ground motion database compiled for nonlinear time-history (NTH) analyses constitutes a representative number of far-fault and near-fault ground motions from a variety of tectonic environments. A total of 14 records were selected to cover a range of frequency content, duration and amplitude. Near-fault records were chosen so as to consider the presence of fling step effects. Hence the assembled database can be investigated in two sub-data sets. The first set contains seven ordinary far-fault ground motions recorded within 90 km of the causative fault plane from earthquakes in the magnitude (M_W) range of 6.5–7.4. The second set includes seven near-fault ground motions characterized with fling step effect. These records are from earthquakes having a magnitude (M_W) range of 6.5–7.4 and are recorded at closest fault distances of 0.0–10km. Information pertinent to the ground motion data sets including station, component of earthquake and peak ground acceleration (PGA), peak ground velocity (PGV), and peak ground displacement (PGD) of records

Table 5. Near-field ground motion database.

NO.	Earthquake	Year	Station	Comp.	M_w	Dis. (km)	PGA (g)	PGV ($cm\,s^{-1}$)	PGD (cm)
1	Kocaeli	1999	Sakarya	90	7.4	3.1	0.37	79.49	70.56
2	Chi-Chi	1999	TCU052	N	7.6	0.24	0.41	118.51	246.27
3	Chi-Chi	1999	TCU052	W	7.6	0.24	0.34	159.04	184.51
4	Chi-Chi	1999	TCU068	N	7.6	1.09	0.46	263.1	430.0
5	Chi-Chi	1999	TCU068	W	7.6	1.09	0.56	176.65	324.27
6	Chi-Chi	1999	TCU072	W	7.6	1.79	0.3	112.47	89.23
7	Chi-Chi	1999	TCU128	W	7.6	9.7	0.139	73.06	90.66

Table 6. Summary of ductility demands for 3-storey building.

Proposed	NSP-4	NSP-3	NSP-1	Demands	Storey
5.1	4.2	3.9	3.4		Total
11.5	9.4	8.4	4.1	Storey	First storey
15.1	13.6	12.2	4.8	Column	
14.4	12.8	11.2	5.0	Beam	
7.1	6.8	6.4	4.8	Storey	Second storey
4.8	4.1	3.0	3.8	Column	
9.1	8.9	9.9	8.3	Beam	
2.4	2.9	3.5	4.9	Storey	Third storey
3.4	4.1	4.8	3.1	Column	
2.7	3.2	3.9	8.0	Beam	

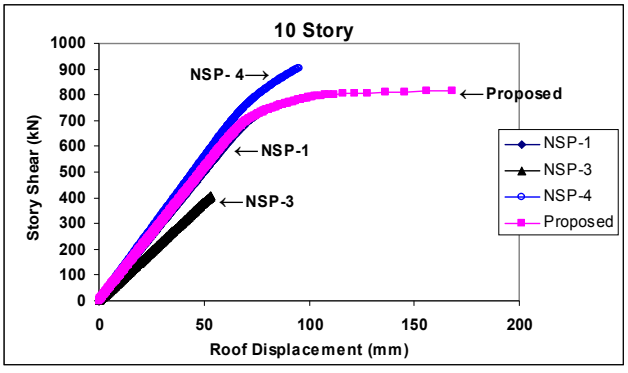

Fig. 15. Base shear vs roof drift response using different lateral load profiles for 10-storey building.

are presented in Tables 4 and 5, and their elastic acceleration response spectra are shown in Figs. 6 and 7.

To facilitate the comparison with pushover analyses, the selected ground motions are scaled so that the resulting peak roof displacement is equal to the target displacement computed for each building. A conventional technique is to scale ground motions such that the spectral acceleration at the fundamental period matches a given design spectrum. The scaling method adopted in this study is based on the FEMA-recommended guideline for the expected peak roof displacement.

7 Evaluation of seismic demands

The estimated demands using the different nonlinear procedures are evaluated at the global and storey levels. Global demands refer to the displacement profile of the building at the peak roof displacement and the base shear vs roof displacement response. At the storey level, the interstorey drift values (relative drift between two consecutive stories) are compared.

7.1 Global demands

To enable direct comparison with demands estimated from the pushover procedure using the four lateral load patterns, estimates of global demand from the NTH analyses for three buildings are shown in Figs. 8 through 10. The mean magnitudes at each storey for each record correspond to the maximum demand at that storey throughout the duration of the event. Section (a) of the figures relates to constant ratio of shear force to building weight and section (b) of the figures relates to constant ratio of roof displacement to building

Table 7. Summary of ductility demands for 6-storey building.

Proposed	NSP-4	NSP-3	NSP-1	Demands	Storey
6.2	5.8	5.2	4.4		Total
11.6	9.6	8.3	5.8	Storey	
12.4	10.6	9.5	6.5	Column	First storey
12.9	11.4	10.7	7.7	Beam	
5.1	5.1	5.1	5.0	Storey	
3.6	2.8	2.5	1.2	Column	Third storey
7.2	6.9	7.2	6.3	Beam	
1.5	2.5	3.4	4.5	Storey	
0.0	0.0	0.0	0.0	Column	Fifth storey
1.7	1.5	3.7	5.4	Beam	

Table 8. Summary of ductility demands for 10-storey building.

Proposed	NSP-4	NSP-3	NSP-1	Demands	Storey
6.4	5.7	5.0	4.5		Total
12.9	11.8	9.6	7.3	Storey	
16.5	13.8	12.6	8.3	Column	First storey
17.2	15.3	12.2	8.4	Beam	
6.8	6.5	6.1	5.8	Storey	
1.7	1.8	1.9	2.3	Column	Third storey
10.0	8.5	7.5	7.7	Beam	
3.6	4.0	4.6	5.4	Storey	
2.3	2.2	2.0	1.4	Column	Fifth storey
3.4	4.4	5.3	7.0	Beam	
–	–	1.1	2.4	Storey	
0.0	0.0	0.0	0.0	Column	Ninth storey
0.0	0.0	1.1	2.6	Beam	

height (recall that ground motions were scaled to produce the same target roof displacement). In most cases, the inverted triangular pattern is found to come closest to the mean time-history estimates of far-field strong motion records. The other three load patterns tend to overestimate or underestimate demands at the lower levels because these patterns typically result in higher loads being applied at the lower floors.

The peak deformed shape along the heights of the buildings shows that the NSP-3 pushover envelope consistently overestimates the peak storey displacements in the low and intermediate storey levels for all buildings and ground motion types investigated, while NSP-2 underestimates the displacements at almost all levels. The NSP-1 and NSP-4 procedures both result in similar estimates and generally yield better estimates of the peak displacement. It is interesting that storey displacement demands from nonlinear static are always conservative for far-fault records. Comparing the time-history responses for the different ground motions indicates that far-fault records generally produce more variability in the demands than near-fault records.

On the other hand, the proposed procedure is shown to predict the drift profiles for all six buildings with relatively better accuracy. The proposed procedure slightly overestimates or underestimates the drift in some cases but captures the overall effects of higher mode contributions more consistently for near-fault records.

7.2 Storey level demands

Interstorey drift has long been recognized as an important indicator of building performance. During an earthquake, the interstorey displacements vary with time as different modes dominate the response. On the other hand, pushover methods which use invariant load patterns produce a consistent pattern of interstorey demand up to initial yielding, following which the storey demands become localized and depend on the storey level to experience first excursion beyond the elastic state.

Interstorey demands are plotted in Figs. 11 through 13 for the three building models. The mean magnitudes at each storey for each record correspond to the maximum demand at that storey throughout the duration of the event. Section (a) of the figures demonstrates constant ratio of shear force to building weight and section (b) of the figures shows constant ratio of roof displacement to building height. The most important observation resulting from the nonlinear time-history evaluation is that the peak storey demands vary from one record to the next. While several earthquakes impose the largest demand at lower levels, there are a number of cases when the largest demands occur at different levels. In general, pushover methods tend to overestimate the storey demands at the lower levels and underestimate them at the upper levels. The discrepancy becomes more apparent with increasing storey height (or longer fundamental periods).

For the entire set of analysed buildings, significant higher mode contributions are evident, resulting in the migration of dynamic drifts from the lower to the upper stories. The NSP-2 methodology grossly underestimates the drifts in upper stories and overestimates them in lower stories, except for the 10-storey building, in which only the lower level demands are captured adequately. Conversely, the NSP-3 always underestimates the drifts at the lower levels and overestimates them at the upper storey levels. NSP-4 and NSP-1 yield better estimates of drift demands compared to NSP-2 and NSP-3. However, in all cases, upper level demands are underestimated by the nonlinear static procedures. On the other hand, the proposed procedure is shown to predict the drift profiles of all four buildings with relatively better accuracy. The proposed procedure slightly overestimates or underestimates the drift in some cases but captures the overall effects of higher mode contributions more consistently for both far-fault and near-fault records.

The uniform distribution which is independent of the earthquake characteristics yields quite different results from other analyses for all response quantities. When the nonlinear dynamic analysis results are taken as reference, it is seen that for constant ratio of roof displacement to building height cases, this distribution yields very high values for floor displacements in all stories of the frame, very low values for storey drift and displacements in constant ratio of shear force to building weight cases. This distribution yields better values only for a few of the bottom stories.

The first mode distribution (NSP-1) which is independent of the earthquake characteristics yields better characteristic results for far-fault records. The higher modes are not very operative on the behaviour of the frame due to frequency content of far-fault records. However, the storey displacements and drifts in the upper stories of the frame cannot be determined by the first mode distribution due to the higher mode effects. In comparison with the other nonlinear procedures, a generalized power distribution yields very high values for floor displacements at all stories of the building. The capacity curves which show the total base shear as a function of the roof drift are displayed in Figs. 14 through 16 for all models. The initial yielding of an element occurs first when using NSP-1. This loading pattern also produces a response with the least system stiffness and the lowest base shear capacity. However, the difference in base shear capacity between the different patterns decreases with storey height. The design base shear of each building is identified in these plots for comparison.

The information generated in Tables 6 through 8 represents the fundamental measures of demand at the global level. The inherent ductility of the system is typically evaluated using the responses shown in Figs. 14 through 16. These plots contain two elements of the reduction (or R factor) used in modern building codes: the difference between first yield of an element and eventual yield of the system contains information on the redundancy in the system while the response beyond the system yield up to the target deformation is a measure of the ductility-based reduction factor.

As seen in Tables 6 through 8, FEMA-356 NSP procedures are not sufficiently accurate for the determination of these ductility demands, and the proposed procedure generally yields better results than FEMA pushover analysis procedures.

8 Conclusions

It has long been recognized that near-fault motions characterized by forward directivity effects are potentially more damaging than far-fault motions, but the consequences of fling-step displacements have not been as well understood. Conventional seismic practice is based on elastic procedures that rely on force reduction factors. Such approaches rely primarily on global demand estimates to evaluate the expected performance of a building. This paper attempts to investigate the validity of nonlinear static approaches to estimate local demands and to explore correlations between storey and global demands. Pushover methods are undoubtedly an improvement over existing elastic force-based procedures and they provide critical information on potential collapse mechanisms and the vulnerability of buildings. For structures responding primarily in the first mode, nonlinear static methods may be a reliable option to estimate inelastic demands. Designing a building to achieve a certain ductility demand can result in much larger demands at the local level. Caution must be exercised when using nonlinear static procedures since the lateral load pattern used to estimate demands can have a significant influence on the computed demands. When compared to nonlinear time-history estimates, pushover methods tend to underestimate demands at the upper levels, signifying the relevance of high mode participation in structures under near-field earthquakes.

Based on this study, an evaluation of the predicted demands (such as peak displacement profile and interstorey

drifts) by the different NSPs forms the basis for the following conclusions:

1. The FEMA-356 method (wherein the envelope of two response measures was considered) provides inadequate predictions of peak interstorey drift at the upper-storey levels when higher mode contributions are significant.

2. Compared to NSP-1 and NSP-3 procedures, NSP-2 provides storey drift estimates that are generally much closer to the mean NTH estimates for far-field earthquakes. However, since the method ignores the inelastic contribution of higher modes, it is unable to reasonably predict demands in the upper stories.

3. It is shown that NSPs based on invariant load vectors using elastic modal properties cannot capture the changes to the dynamic modes resulting from inelastic action. The variation of inertial forces must be considered in static procedures that attempt to reproduce inelastic dynamic response.

4. The proposed procedure provided the best overall match to NTH results. In general, the method is able to reproduce the essential response features, thereby providing a reasonable measure of the likely contribution of higher modes in all phases of the response.

Acknowledgements. The authors would like to express their gratitude to D. Keffer, K. Sasaki and the other anonymous reviewers for their valuable comments and suggestions that improved the manuscript.

Edited by: D. Keefer
Reviewed by: K. Sasaki and two anonymous referees

References

Aydinoglu, M. N.: An incremental response spectrum analysis based on inelastic spectral displacements for multi-mode seismic performance evaluation, Bull.Earthq. Eng., 3–36, 2003.

Aydinoglu, M. N.: An improved pushover procedure for engineering practice: Incremental Response Spectrum Analysis (IRSA), International Workshop on "Performance-based Seismic Design: Concepts and Implementation", Bled, Slovenia 2004, PEER Report 2004/05, 345–356, 2004.

Bracci, J. M., Kunnath, S. K., and Reinhorn, A. M.: Seismic performance and retrofit evaluation of RC structures, J. Struct. Eng., 123, 3–10, 1997.

Chopra, A. K. and Goel, R.: A modal pushover analysis procedure for estimating seismic demands for buildings, Earthq. Eng. Struct. Dynam., 31, 561–582, 2002.

FEMA-356: American Society of Civil Engineers (ASCE), Prestandard and Commentary for the Seismic Rehabilitation of Buildings, prepared for the SAC Joint Venture, published by the Federal Emergency Management Agency, Washington D.C., 2000.

Gulkan, P. and Sozen, M. A.: Inelastic response of reinforced concrete structures to earthquake motions, ACI Structural Journal, 71, 604–610, 1974.

Gupta, B. and Kunnath, S. K.: Adaptive spectra-based pushover procedure for seismic evaluation of structures, Earthq. Spectra, 16, 367–392, 2000.

Huang, K. and Kuang, J. S.: On the applicability of pushover analysis for seismic evaluation of medium- and high-rise buildings, The Structural Design of Tall and Special Buildings, 19, 573–588, 2010.

Iranian Code of Practice for Seismic Resistant Design of Buildings, Standard NO. 2800-05, Building and Housing Research Center, 2005.

Jan, T. S., Liu, M. W., and Kao, Y. C.: An upper-bound pushover analysis procedure for estimating seismic demands of high-rise buildings, Eng. Struct., 26, 117–128, 2004.

Kalkan, E. and Kunnath, S. K.: Adaptive modal combination procedure for nonlinear static analysis of building structures, J. Struct. Eng., 132, 1721–1731, 2006.

Krawinkler, H. and Seneviratna, G. D.: Pros and cons of pushover analysis of seismic performance evaluation, Eng. Struct., 20, 452–464, 1998.

Kunnath, S. K., Reinhorn, A. M., and Lobo, R. F.: IDARC Version 3.0 – a program for inelastic damage analysis of reinforced concrete structures, National Center for Earthquake Engineering Research, Technical Report no. NCEER-92-0022, State University of New York, Buffalo, 1992.

Lefort, T.: Advanced pushover analysis of RC multi-storey buildings, MSc dissertation, Engineering Seismology and Earthquake Engineering Section, Imperial College, London, UK, 2000.

Mao, J., Zhai, C., and Xie, L.: An improved modal pushover analysis procedure for estimating seismic demands of structures, Earthquake Eng. Eng. Vibration, 7, 25–31, 2008.

Mortezaei, A.: Pushover analysis procedure to evaluate seismic demands of buildings under the near-fault ground motions, Report No. SIAU 51284890727005, Semnan branch, Islamic Azad University, Semnan, 2010.

Mwafy, A. M. and Elnashai, A. S.: Static pushover versus dynamic collapse analysis of RC buildings, Eng. Struct., 23, 407–424, 2001.

Pinho, R., Casarotti, C., and Antoniou, S.: A comparison of single-run pushover analysis techniques for seismic assessment of bridges, Earthquake Eng. Struct. Dynam., 36, 1347–1362, 2007.

Sasaki, K. K., Freeman, S. A., and Paret, T. F.: Multimodal pushover procedure (MMP) – a method to identify the effects of higher modes in a pushover analysis, Proceedings of the Sixth US National Conference on Earthquake Engineering, Oakland, California, 1998.

Satyarno, I., Carr, A. J., and Restrepo, J.: Refined pushover analysis for the assessment of older reinforced concrete buildings, Proc. New Zealand National Society for Earthquake Engineering, Technical Conference, Waiarakei, 75–82, 1998.

Somerville, P.: Characterization of near field ground motions, US-Japan Workshop: Effects of Near-Field Earthquake Shaking, San Francisco, 20–21 March 2000.

Tso, W. K. and Moghadam, A. S.: Pushover procedure for seismic analysis of buildings, Prog. Struct. Eng. Materials, 1, 337–344, 1998.

Turker, K. and Irtem, E.: An effective multi-modal and adaptive pushover procedure for buildings, The Bulletin of the Istanbul Technical University, 54, 34–45, 2007.

Wight, J. K., Burak, B., Canbolat, B. A., and Liang, X.: Modeling and software issues in pushover analysis of RC structures, Report Peer-1999/10, US-Japan Workshop on Performance-Based Earthquake Engineering Methodology for Reinforced Concrete Building Structures, Pacific Earthquake Engineering Research Center, Berkeley, CA, 1999.